# Seed-mediated synthesis and the photo-degradation activity of ZnO–graphene hybrids excluding the influence of dye adsorption

Dongying Fu, Gaoyi Han*, Feifei Yang, Tianwen Zhang, Yunzhen Chang, Feifei Liu

*Institute of Molecular Science, Key Laboratory of Chemical Biology and Molecular Engineering of Education Ministry, Shanxi University, Taiyuan 030006, PR China*

## ABSTRACT

The nano-sized ZnO–graphene hybrid has been prepared through combining the facile sol–gel process and hydrothermal method by using $Zn(NO_3)_2 \cdot 6H_2O$ and hexamethylenetetramine (HMT) as growing reactants in the presence of ZnO–graphene oxide (ZnO–GO) seeds. The obtained products have been characterized by X-ray diffraction, scanning electron microscopy, transmission electron microscopy, X-ray photoelectron spectroscopy, Raman spectroscopy and UV–vis absorption spectroscopy. The results show that the GO has been converted to reduced-graphene oxide during the hydrothermal process due to the released reductant from HMT. The photo-degradation of methylene blue in the presence of ZnO–graphene (excluding the influence of the dye adsorption on the catalyst) has also been investigated in detail. It is found that the preparation conditions have significant effects on photo-catalytic properties of the composites, and that ZnO–graphene prepared in the optimal conditions exhibits the optimum activity. This facile and low-cost method will make the composite a perfect candidate in applications of photo-catalysis and other areas.

© 2013 Elsevier B.V. All rights reserved.

## 1. Introduction

Currently, organic dyes and their effluents have become one of the main sources of water pollution, these organic dyes escape from the traditional wastewater treatment and remain in water because of their high stability against light, temperature, chemicals and microbial attack [1,2]. It is expected that photo-catalytic degradation of the organic pollutants can open a new door for the elimination of organic dyes in wastewater [3]. Up to date, it is proved that many semiconductors can be used in photo-degradation of the recalcitrant organic pollutants [3–5]. Among these semiconductors, as a kind of semiconductor widely used in photonic crystals, photo-catalysts, light-emitting diodes, sensors and electroluminescent materials [8], ZnO has got increasing attention because of its suitable band gap of 3.37 eV and the large excitation binding energy (60 meV) at room temperature [4–7]. However, the photo-catalytic efficiency of ZnO has been usually limited by the quick recombination of the photo-generated charge carriers.

During the photo-catalytic degradation, three aspects should be considered: (1) the effective transference of photoelectrons to restrain the recombination of photo-generated electrons and holes; (2) a moderate absorption capacity of the catalyst toward the dye or pollutants; (3) a proper supporting material to support and immobilize the catalyst [9]. Considered the above three aspects, graphene can be used as a promising candidate to support the semiconductor because it possesses the ability to accept the electrons and prevent the recombination, provides a favorable absorption of dye through π–π aggregation between the dye and aromatic regions of graphene, and owns two-dimensional plane and good mechanical intensity to stabilize the catalyst [8–12]. Furthermore, as graphene precursor, graphene oxide (GO) sheets contain various reactive oxygen-containing groups which not only make a good dispersion in aqueous solution but also render fixation of metal or metal oxide particles on the sheets [13–20].

Till now, ZnO has been utilized to decorate graphene sheets to form graphene-supported hybrid with good photo-catalytic properties. For example, Williams and Kamat have fabricated ZnO–graphene composites by using UV-assisted photo-catalytic reduction of GO by ZnO in ethanol solution [21,22]. Li and Cao [23] have reported incorporation of graphene in ZnO to form ZnO–graphene composite by chemically reducing the GO dispersion in aqueous solution by $NaBH_4$, and studied the photo-catalytic performance of the composites for the degradation of rhodamine B under UV and visible light irradiation. Recently, ZnO–graphene composite has also been synthesized by reducing GO coated on the surface of ZnO by hydrazine, and the composites show an improved photo-catalytic efficiency for the degradation of methylene blue

(MB) [24]. Moreover, Wu et al. have presented a general approach for the preparation of sandwich-like graphene/ZnO nanocomposites by solvothermal method in ethylene glycol medium [25]. A microwave-assisted non-aqueous route has also been used to deposit well-dispersed ZnO nanocrystals on reduced graphene oxide sheets with improved photo-activity for the degradation of dyes under visible light [26], and ZnO–graphene composites have been prepared by using a UV-assisted photo-catalytic synthesis [27] and used to enhance photo-catalytic activity in reduction of Cr(VI).

The catalysts supported on graphene and other carbon materials have high adsorption for organic dyes, but the influence of the adsorption of the catalysts for dyes on the photo-catalytic performance has not been thought over till now. In the usual experiments of photo-degradation, dyes with certain concentrations are added into the dispersion of the catalyst initially, the reaction is then traced by measuring the residue of dyes in the solution at certain time interval. The kinetic study of the photo-degradation is generally based on the pseudo-first order reaction, which is reliable when the concentration of the dyes is high enough initially, and well performed when the adsorption of the dye on the catalyst is not strong. But for graphene-supporting catalyst with strong adsorption for dyes, it will show that the photo-degradation rate of dyes is very large although the dye is not degraded so much [28]. Furthermore, the apparent reaction constant of the photo-degradation depends on the light strength, mass of catalyst and the concentration of the dye in the solution etc. Therefore, the influence of the adsorption ability of the catalyst should be considered when the adsorption capacity of the composites is high enough to eliminate most of the dyes since the kinetic constant is determined by measuring the concentration of the dyes in the solution.

In this work, ZnO–graphene composites have been synthesized via combining the facile sol–gel method and seeds growing process at relatively low temperature. The hybrids obtained from this method (low temperature and less time) have been characterized, and their activity of photo-degradation has also been investigated by using almost the same dye concentration in the solution initially in order to exclude the influences of adsorption.

## 2. Experimental

### 2.1. Materials

Natural mineral graphite powder (325 mesh) was obtained from the Tianjin Guangfu Research Institute. The GO was prepared from natural graphite powder according to the previous method [29,30]. Anhydrous ethanol was refluxed over CaO for 2 h and distilled before use. MB was obtained from Zhangjiagang Chemical Plant. Hexamethylenetetramine (HMT), $LiOH \cdot H_2O$, $Zn(NO_3)_2 \cdot 6H_2O$, $Zn(CH_3COO)_2 \cdot 2H_2O$ and other reagents were of analytical grade and used directly without further purification. The GO stock dispersion was prepared by dispersing a certain amount of the GO in ethanol under ultrasonic condition.

### 2.2. Preparation of ZnO–graphene hybrids

ZnO–graphene hybrids were synthesized by two procedures. Firstly, ZnO–GO seeds were synthesized according to the method reported previously [31]. Briefly, 1.10 g (5.0 mmol) $Zn(CH_3COO)_2 \cdot 2H_2O$ was dissolved into 25.0 mL anhydrous ethanol at 80 °C and refluxed under vigorous stirring for about 20 min; after the mixture was cooled to 50 °C, $LiOH \cdot H_2O$ (0.30 g) dissolved in other 25.0 mL anhydrous ethanol containing certain amounts of GO (10, 20, 30, 50 and 75 mg) was slowly added into the solution of $Zn(CH_3COO)_2 \cdot 2H_2O$; the mixture was kept under vigorous stirring for 40 min, in which the resulted ZnO particles were supported on

the surface of the GO sheets, then the mixture was stored at 4 °C overnight after cooling. The synthesized seeds by this procedure were named as ZnO–GO-($n$) ($n$ = 2, 4, 6, 10 and 15) because one fifth of the total seeds were used in one growing solution. Subsequently, the dispersion of ZnO–GO seeds (10.0 mL) was dropped into 200 mL aqueous solution containing equal molar of $Zn(NO_3)_2 \cdot 6H_2O$ and HMT and heated at 90 °C for 3 h in oil bath, during which the ZnO was grown on the seeds and GO was reduced into graphene. Finally, the precipitate containing different amounts of graphene (2, 4, 6, 10 and 15 mg based on the amount of initial addition) was collected by filtering the mixture through the micro-porous filter membrane, washed by deionized water and anhydrous ethanol thoroughly, and then dried at 60 °C under vacuum for 12 h. The ZnO–graphene composites prepared from the growing solution containing 0, 1.0, 3.0, 5.0 and 7.0 mmol $L^{-1}$ $Zn(NO_3)_2 \cdot 6H_2O$ and HMT by using different ZnO–GO as seeds were denoted as ZnO–graphene-($n$)-$m$ ($n$ = 2, 4, 6, 10 and 15; while $m$ = 0, 1, 3, 5 and 7).

### 2.3. Characterization of the samples

The X-ray diffraction (XRD) patterns of the samples were recorded on a Bruker D8 Advance X-ray diffraction meter with Cu Kα radiation and a graphite monochromator at the scan speed of 5° $min^{-1}$ with a step size of 0.02°. The morphologies of the samples were observed by using a JEOL-JSM-6701 field-emission microscope (SEM) operating at an accelerating voltage of 10 kV and a JEOL 2010 transmission electron microscopy (TEM) operating at 200 kV. X-ray photoelectron spectroscopy (XPS) measurements were performed with an ESCAL-ab 220i-XL spectrometer (VG Scientific, England) employing a monochromic Al Kα source at 1486.6 eV, where the binding energies were calibrated by referencing the C1s peak (284.6 eV) to reduce the sample charge effect. Raman spectra were recorded on a Renishaw RM2000 microscopic confocal Raman spectrometer by employing laser of 514 nm as incident light. The measurements of the photo-catalytic activity of the samples and the electron adsorption spectra were carried out on a Varian 50 Bio UV–vis spectrophotometer.

### 2.4. Photocatalytic tests

The photo-degradation process of MB was tracked by using the absorption spectroscopic technique. Firstly, 50.0 mL aqueous solution of MB (20.0 mg $L^{-1}$) containing 30.0 mg of ZnO–graphene was stirred for 30 min in the dark to achieve the adsorption/desorption equilibrium between the catalyst and the dye. The amounts of dye adsorbed on the catalyst were determined by the difference of the absorbance of the MB solution before and after equilibrium. After the MB concentration in the solution was determined, a given amount of the concentrated solution of MB was then added into the mixture to make the absorbance of the solution almost equal to the initial absorbance. Therefore, the concentrations of the dye in solution could be kept enough high before the test of photo-degradation. Subsequently, the mixture was exposed to the light produced by a 200 W Xe lamp under continuously stirring after 5 min equilibrium, the distance between the sample and the lamp was about 36 cm, the temperature was kept at about 25 °C, and the pH of the dispersion was about 6.5 during the process. At a given interval of time, 1.0 mL of suspension was taken out and the concentration of MB was monitored by measuring the absorbance at 650 nm in the mixture of ethanol and water with a volume ration of 3:1 because of the congregation of the MB in pure water [31]. For comparison, experiments were also carried out by using the similar procedure without further addition of MB in the system after 30 min equilibrium. The durability test of the catalyst in the photo-degradation of MB under light radiation was performed following the same procedure, at the beginning, 30.0 mg
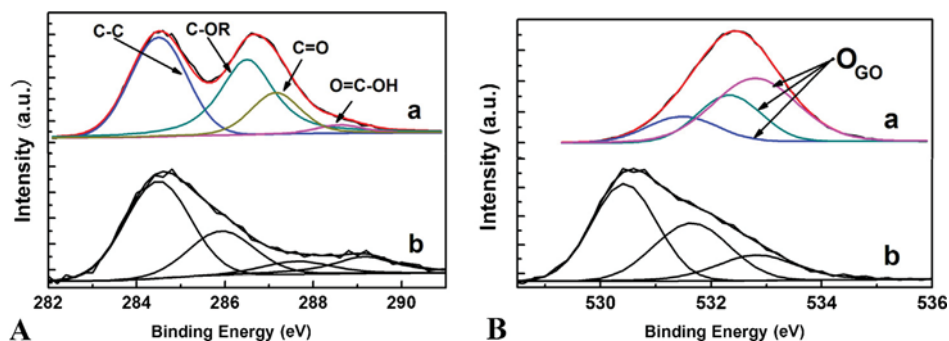
**Fig. 1.** The C1s (A) and O1s (B) XPS spectra of GO and ZnO–graphene-(10)-1. (a) GO and (b) ZnO–graphene-(10)-1.

of the composite was dispersed in 50.0 mL MB solution with the concentration of 20.0 mg L$^{-1}$, and then the mixture underwent five consecutive cycles, each lasting for 50 min. After each cycle, the catalyst was centrifuged and washed thoroughly with water, and then fresh MB solution was added to the catalyst for next time test.

## 3. Results and discussion

### 3.1. The characterization of the samples

The XPS spectra of the GO and ZnO–graphene-(10)-1.have been recorded to identify the valence states of the elements (Fig. 1) in the composites. The curve fitting of the XPS peaks can be performed using Gauss–Lorentzian peak shape after performing a Shirley background correction. The fitted C1s XPS peak of GO at binding energy of 284.6 eV can be attributed to the C—C and C=C bonds, and the peaks at binding energy of 286.5, 287.2 and 288.7 eV are typically assigned to C—OH, C=O and O=C—OH functional groups (Fig. 1A-a), respectively [28,32]. However, the peak intensity related to the oxygen-containing groups has decreased dramatically compared with that related to C—C bonds. It is found that the ratio of the areas related to the C—C and C—O ($R_{cc/co}$) is about 0.75 in the GO spectrum, and that $R_{cc/co}$ increases to about 1.1 in sample of ZnO–graphene-(10)-1. indicating that a considerable degree of oxygen-containing groups in ZnO–GO has been reduced during the hydrothermal process because of the released reductants from HMT. The O1s XPS peak located at 532.4 eV (Fig. 1B-a) is wide and almost symmetric, which can be attributed to the oxygen of hydroxyl and epoxide, carbonyl and carboxyl group in GO [28]. However, the O1s XPS peaks of the samples of ZnO–graphene-(10)-1.are obviously asymmetrical and present a visible shoulder, and the peak centered at 531.8 eV belongs to the lattice oxygen of the ZnO nanoparticles [33].

Raman spectroscopy is considered as a convenient technique to study the ordered/disordered crystal structures of the carbonaceous materials. From the Raman spectra shown in Fig. 2, it is clearly found that GO (Fig. 2 a) shows the D and G bands at 1348 and 1586 cm$^{-1}$. The peak at 2685 cm$^{-1}$ is corresponding to the overtone of the D band, and the peak at 2927 cm$^{-1}$ is associated with the D + G band [32]. The sample of ZnO–graphene (10)-1 presents the similar spectra to GO. The G band is usually attributed to all sp$^2$ carbon forms and provides information on the in-plane vibration of sp$^2$ bonded carbon atoms while the D band suggests the presence of sp$^3$ defects [32]. The ratios of the area of D band to G band ($R_{AD/AG}$) are calculated to be about 2.35 and 2.43 for GO and ZnO–graphene-(10)-1. respectively. This may indicate an increase of the smaller sp$^2$ domains in the composite due to the destruction of the conjugation of the graphene during the reducing process. It is worth noting that a G band up-shift from 1586 to 1599 cm$^{-1}$ is observed for ZnO–graphene-(10)-1.compared with GO, which is
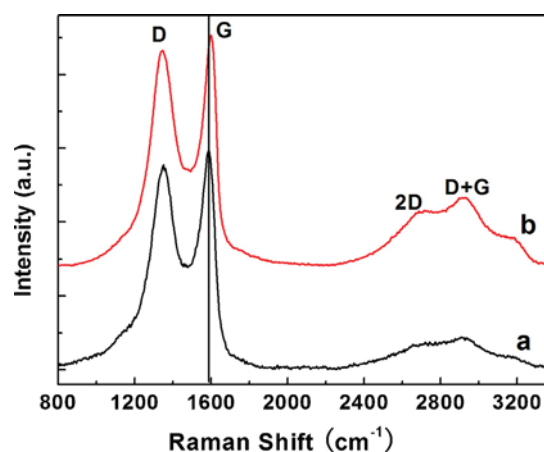


**Fig. 2.** Raman spectra of (a) the graphene oxide (GO), (b) the sample of ZnO–graphene-(10)-1.

generally viewed as an evidence for chemical doping of the carbon materials [34].

The XRD patterns of the ZnO–graphene composites prepared from different conditions are shown in Fig. 3. It is found that all the samples present a typical diffraction character of wurtzite structure according to the standardized JCPDS card (36-1451), which demonstrates that the presence of GO or graphene does not result in the development of new crystal orientations or changes in preferential orientations of ZnO. The average particle sizes can be estimated from (1 0 1) peak by using Debye–Scherrer's formula, it is found that the diameters of the samples are 8.8, 8.2, 9.3, 11.2 and 10.4 nm for ZnO–graphene-(2)-1, ZnO–graphene-(10)-0,



**Fig. 3.** The XRD patterns of the samples of the GO (a), ZnO–graphene-(2)-1 (b), ZnO–graphene -(10)-1 (c), ZnO–graphene-(15)-1 (d), ZnO–graphene- (10)-0 (e) and ZnO–graphene-(10)-7 (f).
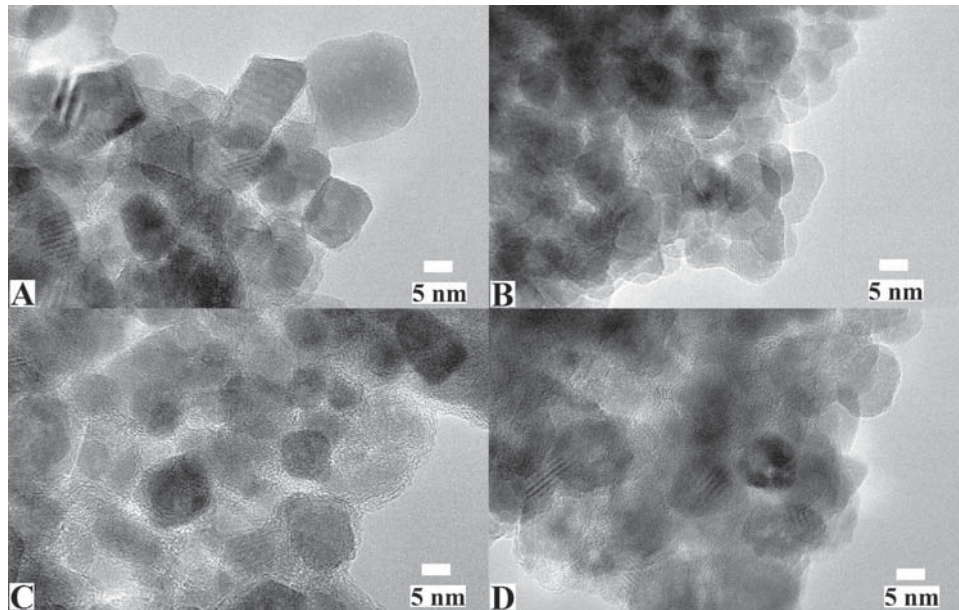
**Fig. 4.** The TEM images of ZnO–graphene-(10)-0 (A), ZnO–graphene-(2)-1 (B) and ZnO–graphene- (10)-1 (C) and ZnO–graphene-(15)-1 (D).

ZnO–graphene-(10)-1, ZnO–graphene-(10)-7 and ZnO–graphene-(15)-1, respectively. The average size of ZnO particles increases with the increment of the concentration of the growing solution when the same ZnO–GO seeds are used, but it also increases with the increase of the content of GO in ZnO-seeds when the same concentration of growing solutions are used. It is easy to understand that the size of the particles increases with the increment of the concentration of growing solution. On the other hand, more GO will aggregate and make the surface area decreased, which will make the ZnO seeds close to each other on the GO surface and cause the size large during the growing process. The characteristic GO peak (Fig. 3a) centered at 11.1° corresponding to the (0 0 1) diffraction [35] has disappeared from the ZnO–graphene composites, which may suggest that the insertion of nanoparticles has exfoliated the GO sheets completely, or that the low amount and low diffraction intensity of graphene cannot make a clear diffraction peak.

From the SEM images of ZnO–graphene composites (Fig. S1), it can be found that the ZnO nanoparticles are densely aggregated together, and that it is not easy to find the graphene sheets in the composites. Furthermore, it is difficult to determine the actual size of ZnO particles owing to their very small size. From the TEM image shown in Fig. 4, it is clear to find that the scale of the ZnO particles is large and the size distribution is not uniform in sample of ZnO–graphene-(10)-0, and that most particles have a size of about 6 nm while some particles even have a size larger than 20 nm (Fig. 4A). The size of ZnO dispersed on the graphene sheets is relatively small and uniform in sample of ZnO–graphene-(2)-1 which has less graphene content (Fig. 4B) although the particles of ZnO exhibit some agglomeration in comparison with other samples. Moreover, it can be clearly found that graphene sheets are decorated by ZnO particles with a quasi-spherical shape and uniform size of about 10 nm (Fig. 4 C) in ZnO–graphene-(10)-1. which is consistent with the data obtained from Scherrer equation. The particles of ZnO are separated from each other and distributed randomly on the graphene sheets, which reveals that there is a good combination between GO sheets and ZnO particles, and indicates that ZnO nanoparticles anchored on graphene facilitate the transfers of electrons upon photo-excitation because the π–π network of graphene is electron acceptor [36]. However, it is strange to find that the particle size of ZnO becomes larger in sample of ZnO–graphene-(15)-1 containing more graphene than others (Fig. 4D), which may be that

the higher concentration of GO facilitates aggregation and makes the surface area decrease during the process of seeds preparation, which makes the nucleation of ZnO close to each other.

From the UV–vis spectra of the composites of ZnO–graphene shown in Fig. S2, it is found that ZnO–graphene-(10)-1.displays an obvious red-shift in the adsorption edge compared with the other composites. The red-shift of the absorption edge increases with the increment of the graphene content in composites due to the interaction between ZnO particles and graphene sheets [37]. Furthermore, the absorbance of ZnO–graphene increases even in visible light region with the increase of the content of graphene in the composites, which is similar to those reported in hybridization of TiO₂ with graphene or other carbon materials [38,39].

### 3.2. Dye adsorption and the photo-catalytic activity of samples

It is well known that the photo-catalytic degradation of the organic pollutants follows the pseudo first-order kinetic [40], which exhibits a linear relationship between $\ln(C_0/C_t)$ and the reaction time. The kinetics equation of the first-order reaction can be described as:

$$\ln \frac{C_0}{C_t} = Kt \tag{1}$$

where $C_0$ is the initial concentration of MB, $t$ the reaction time and $C_t$ the concentration of MB at reaction time of $t$. So based on the first-order equation, the activities of the photo-catalysts are determined by measuring the absorbency of the MB in solution at a certain time intervals.

The adsorption of MB on the composites of ZnO–graphene is strongly influenced by the content of the graphene in the hybrids because of the interaction between the cationic MB and the anionic graphene and the π–π interaction. When we add a certain amount of dye in the dispersion of the catalyst firstly and then the mixture is irradiated by light after adsorption equilibrium according to the method reported previously, it is found that the comparative studies of the photo-catalytic properties of the composites containing different amounts of graphene (especially the samples contain more graphene) become very difficult. For example, the initial absorbance of the MB solution decreases (Fig. 5A) dramatically with the increment of graphene content in ZnO–graphene
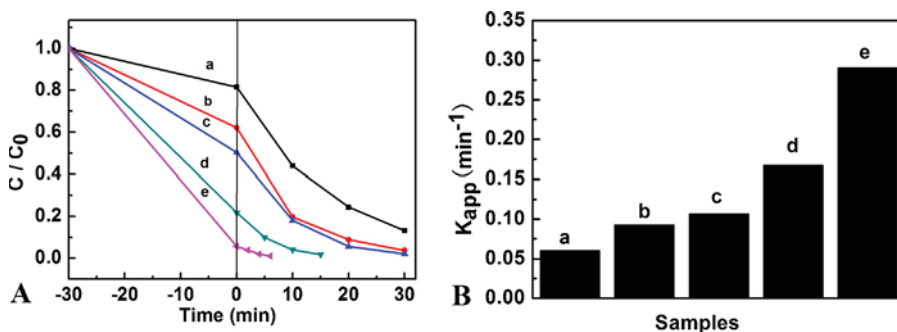
**Fig. 5.** (A) Process of photo-catalytic degradation of MB with different ZnO–graphene composites containing different amounts of graphene (the seeds of Zn–GO are treated in equal molar solution (3 mM) of Zn(NO$_3$)$_2$·6H$_2$O and HMT) and (B) the $K_{app}$ for the photo-catalytic degradation processes of MB. (a) ZnO–graphene-(2)-3, (b) ZnO–graphene-(4)-3, (c) ZnO–graphene-(6)-3, (d) ZnO–graphene-(10)-3 and (e) ZnO–graphene-(15)-3.

composites (the samples are prepared by treating the appropriate seeds in the same amount of growing solution containing 3 mmol L$^{-1}$ Zn(NO$_3$)$_2$·6H$_2$O and HMT). For example, the initial absorbance of the MB solution is found to be only 0.056 when the sample of ZnO–graphene-(15)-3 is used as catalyst. It can be expected that the dye will be adsorbed completely with the content of graphene in the composite increasing further. Moreover, it is interesting to find that the degradation rate of MB also increases with the increment of the graphene content in the composites, for example, it can reach to 100% only after 6 min although the quantity of the degradation MB is very low in the presence of ZnO–graphene-(15)-3 under light irradiation. As seen from Fig. 5B, it is also found that the $K_{app}$ for MB degradation increases with the increase of the graphene content in the composites, which can be deduced that the $K_{app}$ will get very large when most of the dye is adsorbed by the catalyst.

In this case, the value of $K_{app}$ obtained from pseudo first-order kinetic will be not accurate when the concentration of the substrates is lower than some extent because the pseudo first-order kinetic requires one reactant more than ten times than the other in the homogeneous reaction. Therefore, the influence of the adsorption ability of the catalyst should be considered when the adsorption ability of the composites is high enough to eliminate most of the dyes since the kinetic constant is determined by measuring the concentration in the solution. So we use a certain amount of ZnO–graphene composites as catalyst to disperse in the solution of MB (the absorbance of the solution of MB is measured initially), after the mixture has been stirred for 30 min under dark to get the adsorption equilibrium, then amount of MB concentrated solution (1.0 mg mL$^{-1}$) is added into the mixture to make the concentration of MB in the solution maintaining a range for the photo-degradation. Thus, the degradation of the dye is carried out in approximately the same conditions, so the true activity of

the catalyst can be reflected due to excluding the influence of the adsorption.

Using the modified method, it is clearly found (Fig. 6A) that the $K_{app}$ value of MB degradation increases with the increase of the content of graphene in the composites initially, while it decreases with the increment of graphene content in the composites further after the value of $K_{app}$ reaches to the maximum of 0.07176 min$^{-1}$ for the sample of ZnO–graphene-(10)-1.which is prepared by using ZnO–GO-(10) as the seeds in 1.0 mmol L$^{-1}$ growing solution. This is because the black graphene in the composites will increase the light absorbing and scattering, leading to a decrease of the photo-catalytic activity of the composites when the graphene content is too high [9]. Another reason is that the excessive graphene can act as a kind of recombination center to promote the recombination of electron hole pair in graphene [41]. The typical electron adsorption spectra of the MB after irradiating by light for different time are shown in Fig. 6B, it is clear that the absorbance of the MB decreases dramatically with the increment of the irradiation time. Furthermore, it is found that the photo-degradation of MB in the presence of ZnO–graphene-(10)-1.follows the first-order equation (inserted figure in Fig. 6B).

Using ZnO–GO-(10) as seeds, the composites of ZnO–graphene-(10)-m have been prepared in the growing solution containing various concentrations of Zn(NO$_3$)$_2$·6H$_2$O and HMT, and used as catalysts to degrade the MB. It is found that the photo-catalytic activities of the composites (Fig. 7) are obviously influenced by the concentrations of the growing solution, which indicates that the concentration of reactants in the growing solution can be used to adjust the properties of ZnO–graphene during the process of preparation. Combining the Figs. 6 and 7, it can be found that the ZnO–graphene exhibits the maximum $K_{app}$ when the seeds of ZnO–GO-(10) are treated by the growing solution containing 1.0 mM reactants.
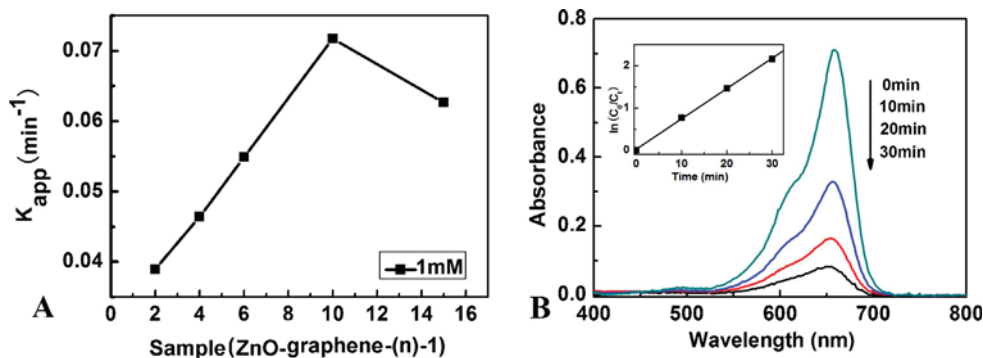


**Fig. 6.** The plot of $K_{app}$ versus ZnO–graphene composites prepared from different seeds of ZnO–GO-(n, n = 2, 4, 6, 10 and 15) in 1 mM growing solution (A) and the adsorption spectra of MB during the photo-degradation with ZnO–graphene (10)-1 (inserted figure: the relationship between ln($C_0/C_t$) and time) (B).
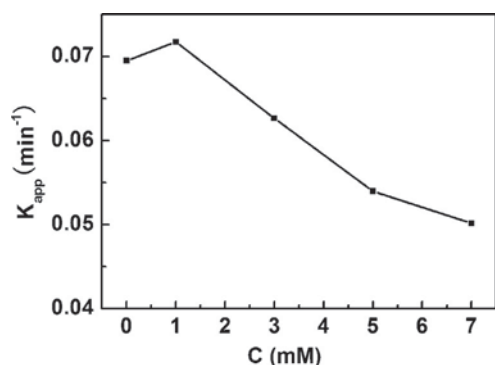
**Fig. 7.** Effect of the ZnO–graphene composites prepared from different concentrations of reactants $(Zn(NO_3)_2 \cdot 6H_2O$ and HMT) by using the same seeds of ZnO–GO-(10).
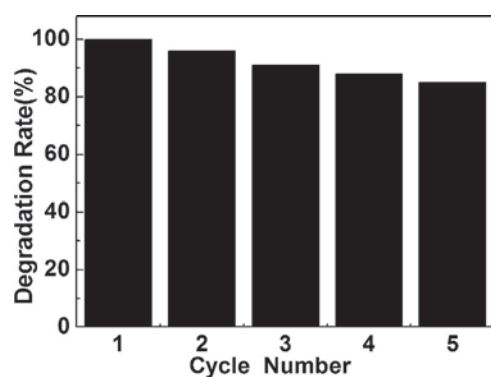


**Fig. 8.** The influence of catalyst use number of times on activeness of photochemical catalyst of ZnO–GO-(10)-1.

The cyclic properties of the catalyst are also measured in 50 mL MB solution $(20\,mg\,L^{-1})$ containing 30 mg ZnO–GO-(10)-1.using the similar method. Keeping the condition of photo-catalytic degradation invariable, the identical catalyst is to be used 1, 2, 3, 4, 5 times separately under the radiation of 50 min each time. From the results shown in Fig. 8, changes of degradation rate are observed from the relationship between the number of times of reuse and the photodegradation rate. The experiments indicate that the composite of ZnO–GO-(10)-1.can still retain 85% activity for degradation of MB after repeated uses of 5 times, indicating that it can be reused.

## 4. Conclusions

In summary, the nano-sized ZnO–graphene hybrids have been prepared by combining the facile sol–gel and hydrothermal seeds-growing methods. The photo-degradation of MB in the presence of ZnO–graphene composites has been investigated by excluding the adsorption of dye on the catalysts. Through controlling the concentration of reactant and the content of GO, it is found that the preparation conditions have a significant effect on photo-catalytic properties of the composites. The ZnO–graphene prepared by using 1.0 mM growing solution to treat ZnO–GO-(10) seeds exhibits the optimum activity. The obtained ZnO–graphene composites have a potential application in water purification.

## Acknowledgements

## Appendix A. Supplementary data

Supplementary data associated with this article can be found, in the online version, at http://dx.doi.org/10.1016/j.apsusc.2013.07.003

## References

[1] I. Arslan, I.A. Balcioglu, T. Tuhkanen, D. Bahnemann, J. Environ. Eng. 126 (2000) 903–911.
[2] E. Forgacs, T. Cserhati, G. Oros, Environ. Int. 30 (2004) 953–971.
[3] M.R. Hoffmann, S.T. Martin, W.Y. Choi, D.W. Bahnemannt, Chem. Rev. 95 (1995) 69–96.
[4] W. Yao, X. Fang, D.F. Guo, Z.Y. Gao, D.P. Wu, K. Jiang, Appl. Surf. Sci. 274 (2013) 39–44.
[5] M.H. Huang, S. Mao, H. Feick, H. Yan, Y. Wu, H. Kind, E. Weber, R. Russo, P. Yang, Science 292 (2001) 1897–1899.
[6] M. Fu, Y.L. Li, S.W. Wu, P. Lu, J. Liu, F. Dong, Appl. Surf. Sci. 258 (2011) 1587–1591.
[7] Z. Cao, Z.J. Zhang, Appl. Surf. Sci. 257 (2011) 4151–4158.
[8] S.J. Pearton, D.P. Norton, K. Ip, Y.W. Heo, T. Steiner, Prog. Mater. Sci. 50 (2005) 293–340.
[9] G.D. Jiang, Z.F. Lin, C. Chen, L.H. Zhu, Q. Chang, N. Wang, W. Wei, H.Q. Tang, Carbon 49 (2011) 2693–2701.
[10] H.L. Guo, X.F. Wang, Q.Y. Qian, F.B. Wang, X.H. Xia, ACS Nano 3 (2009) 2653–2659.
[11] Y. Zhou, Q. Bao, L.A.L. Tang, Y. Zhong, K.P. Loh, Chem. Mater. 21 (2009) 2950–2956.
[12] D. Li, M.B. Muller, S. Gilje, R.B. Kaner, G.G. Wallace, Nat. Nanotechnol. 3 (2008) 101–105.
[13] K.S. Novoselov, A.K. Geim, S.V. Morozov, D. Jiang, M.I. Katsnelson, I.V. Grigorieva, S.V. Dubonos, A.A. Firsov, Nature 438 (2005) 197–200.
[14] S. Stankovich, D.A. Dikin, G.H.B. Dommett, K.M. Kohlhaas, E.J. Zimney, E.A. Stach, Nature 442 (2006) 282–286.
[15] N.A. Kotov, Nature 442 (2006) 254–255.
[16] S. Watcharotone, D.A. Dikin, S. Stankovich, R. Piner, I. Jung, G.H.B. Dommett, G. Evmenenko, S.E. Wu, S.F. Chen, C.P. Liu, S.T. Nguyen, R.S. Ruoff, Nano Lett. 7 (2007) 1888–1892.
[17] D. Wang, D. Choi, J. Li, Z. Yang, Z. Nie, R. Kou, C.M. Wang, L.V. Saraf, J.G. Zhang, I.A. Aksay, J. Liu, ACS Nano 3 (2009) 907–914.
[18] A.P. Yu, P. Ramesh, M.E. Itkis, E. Bekyarova, R.C. Haddon, J. Phys. Chem. C 111 (2007) 7565–7569.
[19] I.V. Lightcap, T.H. Kosel, P.V. Kamat, Nano Lett. 10 (2010) 577–583.
[20] A. Mukherji, B. Seger, G.Q. Lu, L. Wang, ACS Nano 5 (2011) 3483–3492.
[21] G. Williams, P.V. Kamat, Langmuir 25 (2009) 13869–13873.
[22] O. Akhavan, Carbon 49 (2011) 11–18.
[23] J. Li, H.Q. Cao, J. Mater. Chem. 21 (2011) 3346–3349.
[24] T.G. Xu, L.W. Zhang, H.Y. Cheng, Y.F. Zhu, Appl. Catal. B: Environ. 101 (2011) 382–387.
[25] J.L. Wu, X.P. Shen, L. Jiang, K. Wang, K.M. Chen, Appl. Surf. Sci. 256 (9) (2010) 2826–2830.
[26] Y. Liu, Y. Hu, M.J. Zhou, H.S. Qian, X. Hu, Appl. Catal. B: Environ. 125 (2012) 425–431.
[27] X.J. Liu, L.K. Pan, Q.F. Zhao, T.L.G. Zhu, T.Q. Chen, T.L.Z. Sun, C.Q. Sun, Chem. Eng. J. 183 (2012) 238–243.
[28] J.C. Liu, H.W. Bai, Y.J. Wang, Z.Y. Liu, X.W. Zhang, D.D. Sun, Adv. Funct. Mater. 20 (2010) 4175–4181.
[29] Y.X. Xu, H. Bai, G.W. Lu, C. Li, G.Q. Shi, J. Am. Chem. Soc. 130 (2008) 5856–5857.
[30] Y.X. Xu, Q. Wu, Y.Q. Sun, H. Bai, G.Q. Shi, ACS Nano 4 (2010) 7358–7362.
[31] D.Y. Fu, G.Y. Han, Y.Z. Chang, J.H. Dong, Mater. Chem. Phys. 132 (2012) 673–681.
[32] F. Wang, K. Zhang, J. Mol. Catal. A: Chem. 345 (2011) 101–107.
[33] X.G. Han, H.Z. He, Q. Kuang, X. Zhou, X.H. Zhang, T. Xu, Z.X. Xie, L.S. Zheng, J. Phys. Chem. C 113 (2009) 584–589.
[34] E.P. Gao, W.Z. Wang, M. Shang, J.H. Xu, Phys. Chem. Chem. Phys. 13 (2011) 2887–2893.
[35] S. Zhang, Y. Shao, H. Liao, M.H. Engelhard, G. Yin, Y. Lin, ACS Nano 5 (2011) 1785–1791.
[36] Y.J. Yokomizo, S. Krishnamurthy, P.V. Kamat, Catal. Today 199 (2013) 36–41.
[37] Y. Zhang, Z.R. Tang, X. Fu, Y.J. Xu, ACS Nano 4 (2010) 7303–7314.
[38] Y.J. Wang, R. Shi, J. Lin, Y.F. Zhu, Appl. Catal. B: Environ. 100 (2010) 179–183.
[39] K. Zhou, Y. Zhu, X. Yang, X. Jiang, C. Li, New J. Chem. 35 (2011) 353–359.
[40] Y.J. Li, X.D. Li, J.W. Li, J. Yin, Water Res. 40 (2006) 1119–1126.
[41] G. Zhu, T. Xu, T. Lv, L.K. Pan, Q.F. Zhao, Z. Sun, J. Electroanal. Chem. 650 (2011) 248–251.